

RM
A53/2

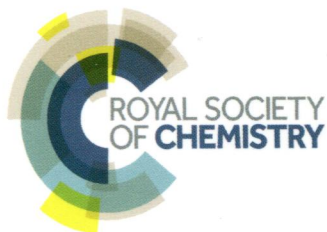
Volume 139 | Number 24 | 21 December 2014 | Pages 6313–6592

Analyst

www.rsc.org/analyst



ISSN 0003-2654

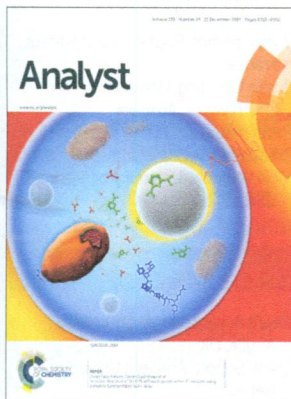


PAPER

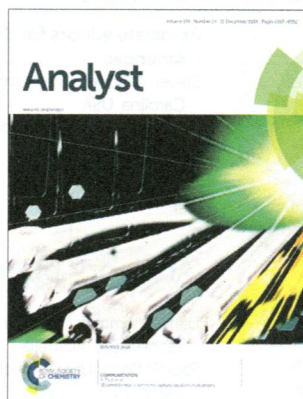
Stuart Farquharson, Jason Guicheteau *et al.*
Selective detection of 1000 *B. anthracis* spores within 15 minutes using
a peptide functionalized SERS assay

IN THIS ISSUE

ISSN 0003-2654 CODEN ANALAO 139(24) 6313–6592 (2014)



Cover
See Stuart Farquharson,
Jason Guicheteau *et al.*,
pp. 6366–6370.
Image reproduced by
permission of Stuart
Farquharson from *Analyst*,
2014, 139, 6366.



Inside cover
See B. Paull *et al.*,
pp. 6343–6347.
Image reproduced by
permission of B. Paull from
Analyst, 2014, 139, 6343.

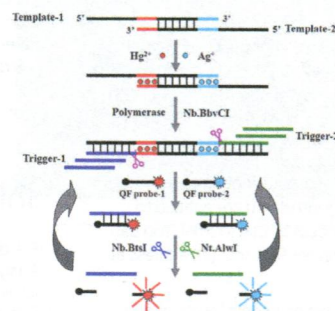
CRITICAL REVIEW

6326

Functional nucleic acid-based sensors for heavy metal ion assays

Guichi Zhu and Chun-yang Zhang*

This review summarizes the development and the trends of functional nucleic acid-based sensors for various heavy metal ion assays.



COMMUNICATIONS

6343

3D printed metal columns for capillary liquid chromatography

S. Sandron, B. Heery, V. Gupta, D. A. Collins,
E. P. Nesterenko, P. N. Nesterenko, M. Talebi, S. Beirne,
F. Thompson, G. G. Wallace, D. Brabazon, F. Regan
and B. Paull*

3D printing of metal alloys, both stainless steel and titanium, has been used for the creation of long capillary columns (600 mm) within small footprint designs (30 mm × 58 mm) for use in high-pressure liquid chromatography applications.



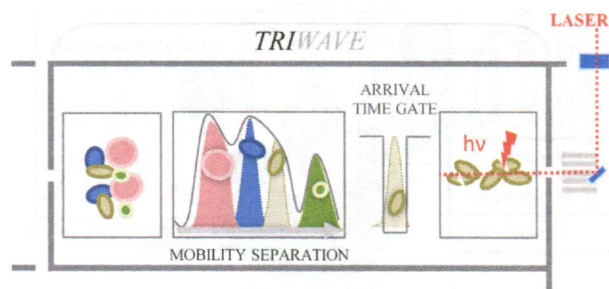
Федеральное государственное
бюджетное учреждение науки
Центральная научная библиотека
Уральского отделения
Российской академии наук (ЦНБ УрО РАН)

6348

UV photodissociation of trapped ions following ion mobility separation in a Q-ToF mass spectrometer

Bruno Bellina, Jeffery. M. Brown, Jakub Ujma, Paul Murray, Kevin Giles, Michael Morris, Isabelle Compagnon* and Perdita. E. Barran*

An ion mobility mass spectrometer has been modified to allow optical interrogation of ions with different mass-to-charge ratios and/or mobilities.

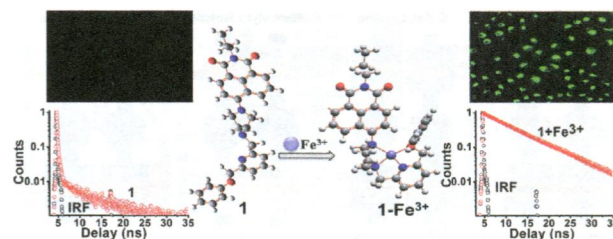


6352

A naphthalimide based PET probe with Fe^{3+} selective detection ability: theoretical and experimental study

Narendra Reddy Chereddy,* M. V. Niladri Raju, Peethani Nagaraju, Venkat Raghavan Krishnaswamy, Purna Sai Korrapati, Prakriti Ranjan Bangal* and Vaidya Jayathirtha Rao*

A naphthalimide based Fe^{3+} selective fluorescence 'turn-on' probe that operates based on a PET mechanism has been synthesized, and its application in the detection of Fe^{3+} ions in aqueous samples and in live cells is explored.

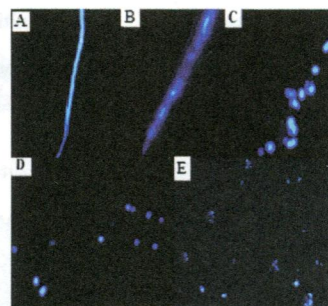


6357

Characterization of Cr(v)-induced genotoxicity using CdTe nanocrystals as fluorescent probes

Wen-Hao Zhang,* Chao-Xia Sui, Xie Wang, Gong-Ju Yin, Ying-Fan Liu* and Ding Zhang

A stepwise process of Cr(v)-induced DNA breakage incubated for different times under an inverted fluorescence microscope.

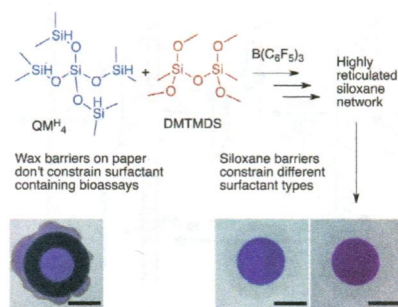


6361

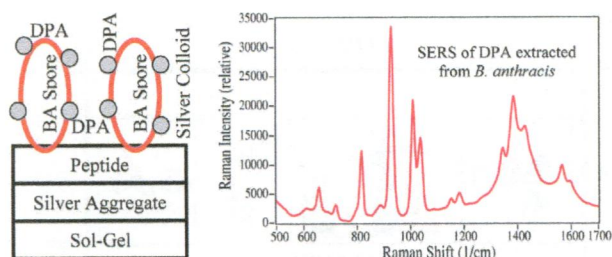
Printing silicone-based hydrophobic barriers on paper for microfluidic assays using low-cost ink jet printers

Vinodh Rajendra, Clémence Sicard, John D. Brennan and Michael A. Brook*

Inkjet printed silicone resins provide hydrophobic barriers for paper-based microfluidic assays.



6366

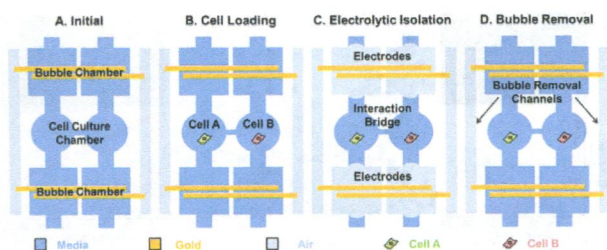


Selective detection of 1000 *B. anthracis* spores within 15 minutes using a peptide functionalized SERS assay

Stuart Farquharson,* Chetan Shende, Wayne Smith, Hermes Huang, Frank Inscore, Atanu Sengupta, Jay Sperry, Todd Sickler, Amber Prugh and Jason Guicheteau

We developed a SERS assay that allowed selective detection of 1000 *B. anthracis* Ames spores in less than 15 minutes using dipicolinic acid (DPA) as a biomarker.

6371

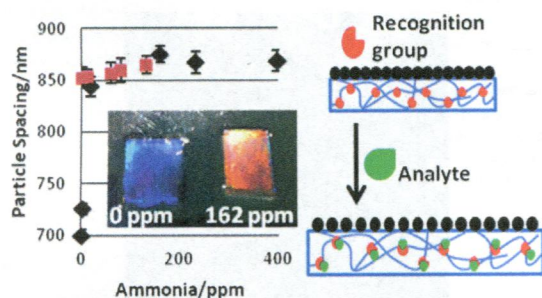


Electrolytic valving isolation of cell co-culture microenvironment with controlled cell pairing ratios

Yu-Chih Chen,* Patrick Ingram and Euisik Yoon*

Cancer–stromal interaction is a critical process in tumorigenesis.

6379

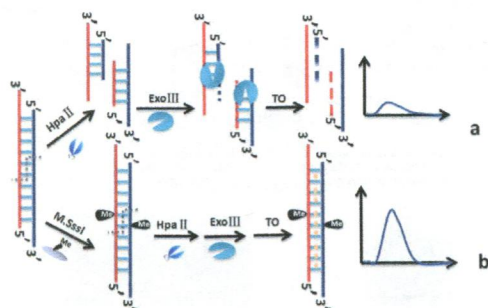


Responsive ionic liquid–polymer 2D photonic crystal gas sensors

Natasha L. Smith, Zhenmin Hong and Sanford A. Asher*

Responsive polymer–ionic liquid systems that are stable with respect to ambient conditions and capable of detecting gases.

6387



Label-free fluorescence detection of DNA methylation and methyltransferase activity based on restriction endonuclease *HpaII* and exonuclease III

Chunyan Gao, Henan Li, Yuanjian Liu, Wei Wei,* Yuanjian Zhang and Songqin Liu

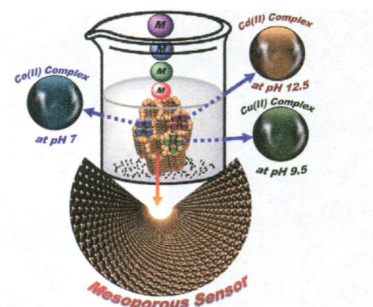
The principle of label-free fluorescence detection of site-specific DNA methylation and *M.SssI* MTase activity based on *HpaII* and Exo III is reported.

6393

Monolithic scaffolds for highly selective ion sensing/removal of Co(II), Cu(II), and Cd(II) ions in water

Mohamed A. Shenashen, Sherif A. El-Safty* and Emad A. Elshehy

Optical sensor mesostructures enabled the selective recognition, removal, and extraction of multiple metal ions from water samples with unique sensing properties.

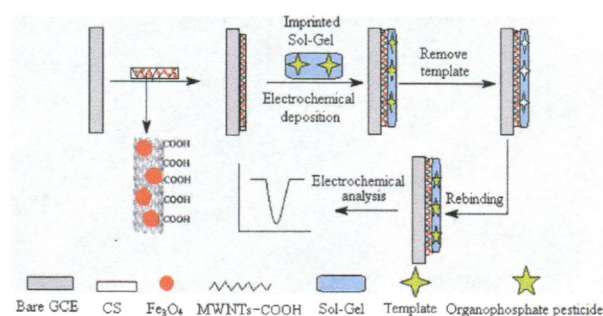


6406

Development of molecularly imprinted electrochemical sensors based on Fe₃O₄@MWNT-COOH/CS nanocomposite layers for detecting traces of acephate and trichlorfon

Qinghua Tang, Xiujuan Shi, Xiaolin Hou, Jie Zhou and Zhixiang Xu*

In this study, we developed a novel biomimetic electrochemical imprinted sensor sensitized with a Fe₃O₄@MWNT-COOH/CS nanocomposite layer for the rapid detection of acephate and trichlorfon.

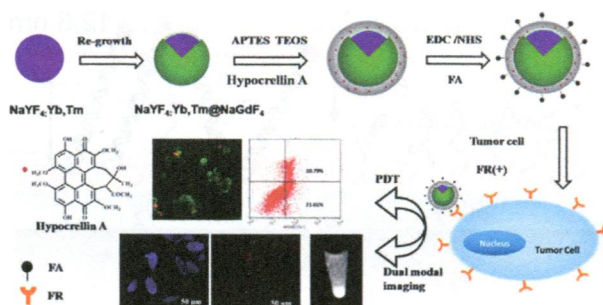


6414

Dual-modal imaging and photodynamic therapy using upconversion nanoparticles for tumor cells

Chunna Yang, Qiuling Liu, Dacheng He, Na Na, Yunling Zhao and Jin Ouyang*

Schematic of the design of the multifunctional nanocomposites.

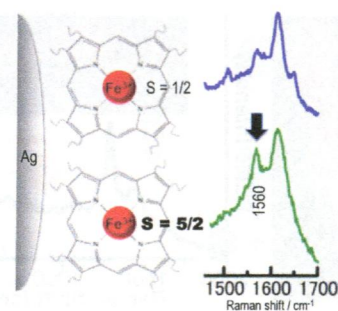


6421

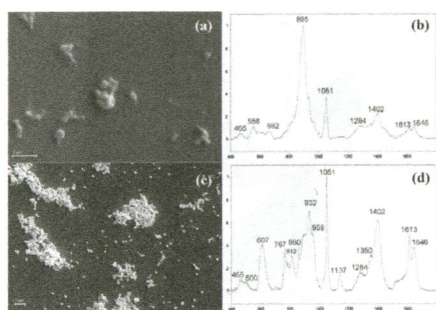
Sensitive marker bands for the detection of spin states of heme in surface-enhanced resonance Raman scattering spectra of metmyoglobin

Yasutaka Kitahama,* Masatoshi Egashira, Toshiaki Suzuki, Ichiro Tanabe and Yukihiro Ozaki

The SERRS intensity ratio of the peak at 1560 cm⁻¹ to that at 1620 cm⁻¹ was applied to detect the spin states of heme in metmyoglobin sensitively.



6426

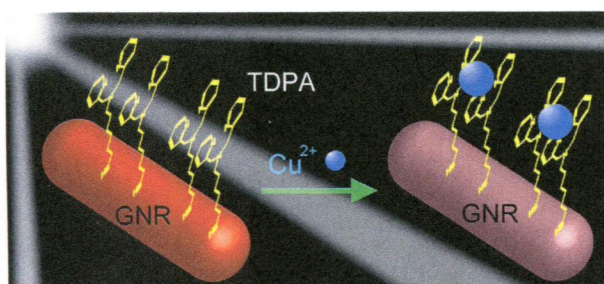


The multivariate detection limit for *Mycoplasma pneumoniae* as determined by nanorod array-surface enhanced Raman spectroscopy and comparison with limit of detection by qPCR

Kelley C. Henderson, Edward S. Sheppard, Omar E. Rivera-Betancourt, Joo-Young Choi, Richard A. Dluhy, Kathleen A. Thurman, Jonas M. Winchell and Duncan C. Krause*

The detection limits by NA-SERS and qPCR for the bacterial pathogen *Mycoplasma pneumoniae* were compared.

6435

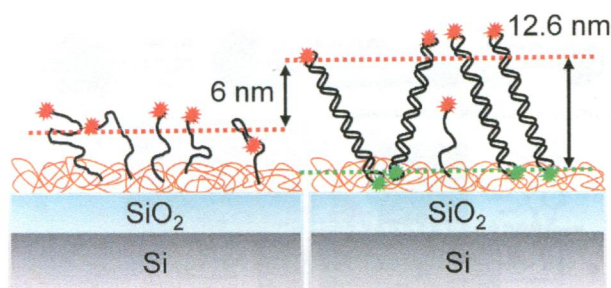


A single gold nanorod as a plasmon resonance energy transfer based nanosensor for high-sensitivity Cu(II) detection

Chao Jing, Lei Shi, Xiaoyuan Liu and Yi-Tao Long*

Plasmon resonance energy transfer (PRET) has been widely applied in the detection of bio-recognition, heavy metal ions and cellular reactions with high sensitivity, based on the overlap between the plasmon resonance scattering band of nanoparticles and the absorption band of the surface-modified chromophore molecules.

6440

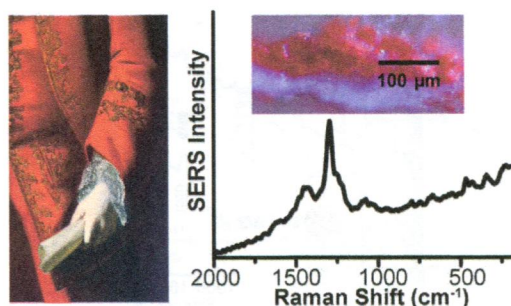


Nanoscale characterization of DNA conformation using dual-color fluorescence axial localization and label-free biosensing

Xirui Zhang, George G. Daaboul, Philipp S. Spuhler, David S. Freedman, Abdulkadir Yurt, Sunmin Ahn, Oguzhan Avci and M. Selim Ünlü*

Simultaneous quantification of surface density and conformation of surface-immobilized DNA on a layered substrate functionalized with 3-D polymeric coating.

6450



Combined SERS and Raman analysis for the identification of red pigments in cross-sections from historic oil paintings

Kristen A. Frano, Hannah E. Mayhew, Shelley A. Svoboda and Kristin L. Wustholz*

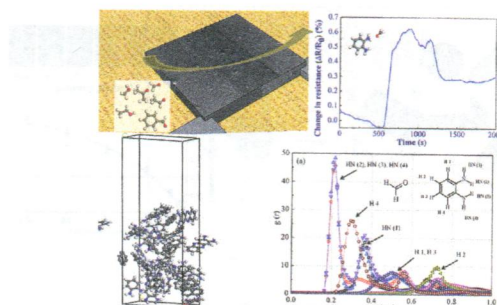
SERS and normal Raman approach to identify red pigments in cross-sections from historic oil paintings.

6456

Investigation of selective sensing of a diamine for aldehyde by experimental and simulation studies

Ashwini N. Mallya and Praveen C. Ramamurthy*

An organic molecule – *o*-phenylene diamine (OPD) – is selected as an aldehyde sensing material.

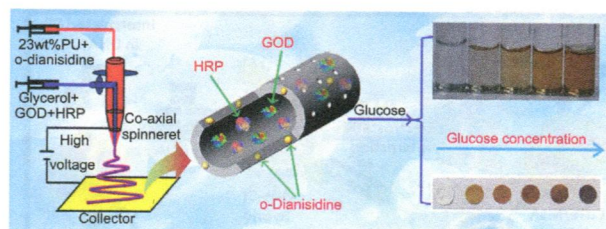


6467

"Ready-to-use" hollow nanofiber membrane-based glucose testing strips

Xiaoyuan Ji, Zhiguo Su, Ping Wang, Guanghui Ma and Songping Zhang*

Fabrication and application of a hollow nanofiber membrane-based test strip for glucose detection.

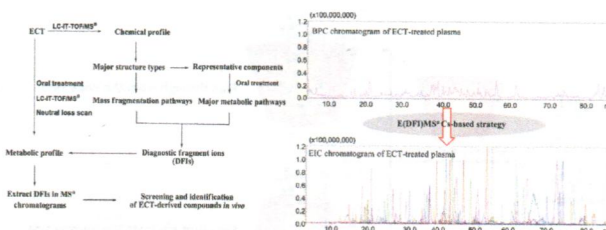


6474

Characterization of the herb-derived components in rats following oral administration of *Carthamus tinctorius* extract by extracting diagnostic fragment ions (DFIs) in the MSⁿ chromatograms

Jin-Feng Chen, Yue-Lin Song, Xiao-Yu Guo, Peng-Fei Tu and Yong Jiang*

An E(DFI)MSⁿCs-based strategy was proposed to rapidly detect and identify the *in vivo* components derived from the extract of *Carthamus tinctorius* using LC-IT-TOF-MSⁿ.

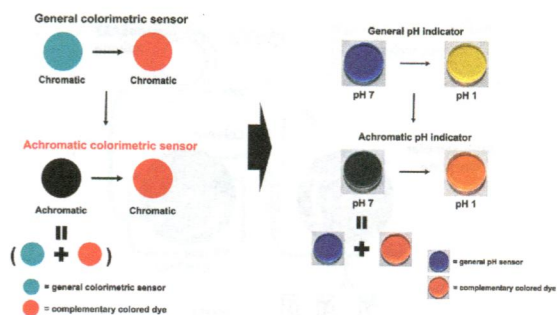


6486

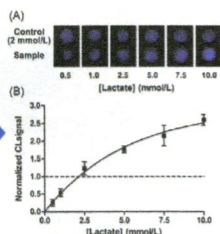
Achromatic–chromatic colorimetric sensors for on–off type detection of analytes

Jun Hyuk Heo, Hui Hun Cho, Jin Woong Lee and Jung Heon Lee*

We developed a method to convert a general colorimetric sensor to an achromatic colorimetric sensor by introducing a complementary colored dye to the sensor, helping users to detect the presence of analytes at much lower concentration and recognize the existence of analytes instinctively.



6494

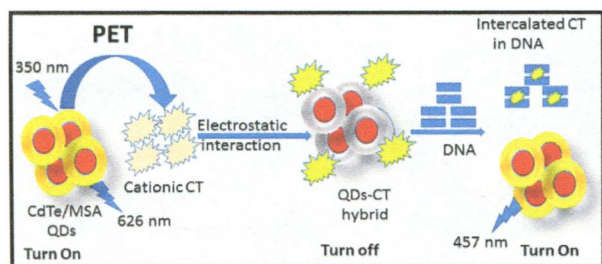


A 3D-printed device for a smartphone-based chemiluminescence biosensor for lactate in oral fluid and sweat

Aldo Roda,* Massimo Guardigli, Donato Calabria, Maria Maddalena Calabretta, Luca Cevenini and Elisa Micheli

Smartphone-based chemiluminescence biosensor for lactate detection.

6502

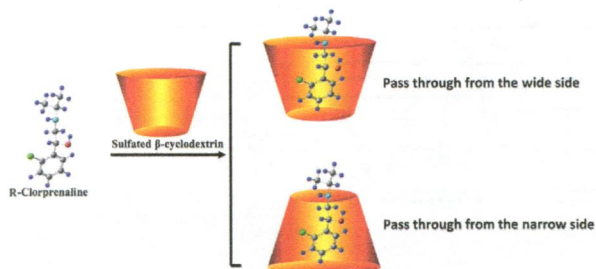


A supramolecular nanobiological hybrid as a PET sensor for bacterial DNA isolated from *Streptomyces sanglieri*

Sudesna Chakravarty, Dilip Saikia, Priyanka Sharma, Nirab Chandra Adhikary, Debajit Thakur and Neelotpal Sen Sarma*

A 'turn on-off-on' sensor for highly sensitive detection of ds DNA with an excellent 'limit of detection' is reported.

6511



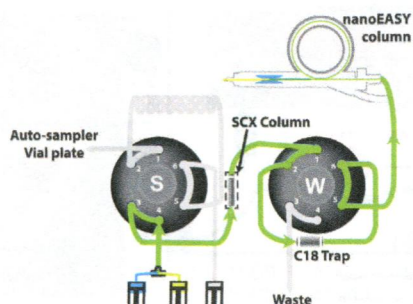
Process of complexation for R-Clorprenaline with sulfated β -cyclodextrin

Quantitative prediction of enantioseparation using β -cyclodextrin derivatives as chiral selectors in capillary electrophoresis

Xin Guo, Zhiqiang Wang, Lihua Zuo, Zhixu Zhou, Xingjie Guo* and Tiemin Sun*

A specific value of interaction energy difference which can be used to predict the possibility of enantioseparation before CE experiments was discovered.

6520



Characterization and usage of the EASY-spray technology as part of an online 2D SCX-RP ultra-high pressure system

Fabio Marino, Alba Cristobal, Nadine A. Binai, Nicolai Bache, Albert J. R. Heck* and Shabaz Mohammed*

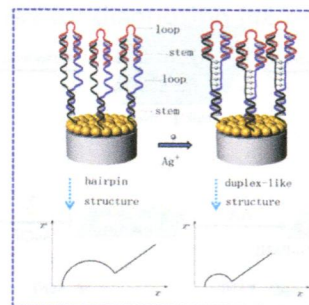
The EASY-spray technology can now be implemented as a simple online 2D SCX-RP ultra-high pressure system, which allows one to reach deep proteome coverages.

6529

Sensitive impedimetric biosensor based on duplex-like DNA scaffolds and ordered mesoporous carbon nitride for silver(I) ion detection

Yaoyu Zhou, Lin Tang,* Xia Xie, Guangming Zeng,* Jiajia Wang, Yaocheng Deng, Guide Yang, Chen Zhang, Yi Zhang and Jun Chen

An unlabeled immobilized DNA-based biosensor with MCN for the detection of Ag^+ by EIS with $[\text{Fe}(\text{CN})_6]^{4-/3-}$ as a redox couple.

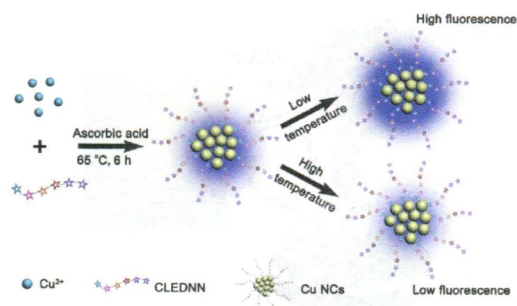


6536

Green synthesis of peptide-templated fluorescent copper nanoclusters for temperature sensing and cellular imaging

Hong Huang, Hua Li, Ai-Jun Wang,* Shu-Xian Zhong, Ke-Ming Fang and Jiu-Ju Feng*

We have developed a simple and green method for synthesis of blue fluorescent peptide-templated Cu nanoclusters (NCs) which display temperature dependence fluorescence and low toxicity as a probe for temperature sensing and cellular imaging.

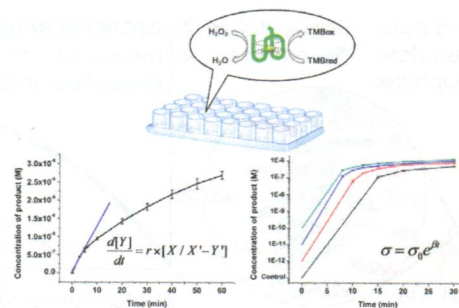


6542

A G-quadruplex based platform for label-free monitoring of DNA reaction kinetics

Ji Nie, Liang-Yuan Cai, Fang-Ting Zhang, Ming-Zhe Zhao, Ying-Lin Zhou* and Xin-Xiang Zhang*

For the first time, a G-quadruplex based platform was established for the simple, label-free, rapid and high-throughput monitoring of DNA reaction kinetics.

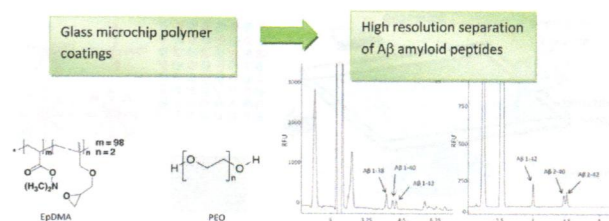


6547

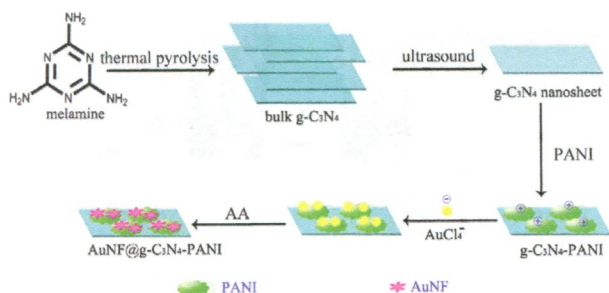
Neutral polymers as coatings for high resolution electrophoretic separation of A β peptides on glass microchips

Kiarach Mesbah, Romain Verpillot, Marcella Chiari, Antoine Pallandre and Myriam Taverna*

EpDMA, an efficient coating for glass microchip to achieve high resolution separation of relevant A β peptides for Alzheimer's disease diagnosis.



6556

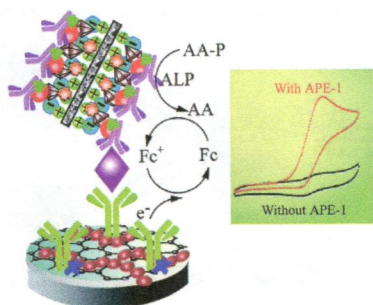


Enhanced electrochemiluminescence sensor for detecting dopamine based on gold nanoflower@g-graphitic carbon nitride polymer nanosheet–polyaniline hybrids

Qiyi Lu, Juanjuan Zhang, Xiaofang Liu, Yuanya Wu, Ruo Yuan* and Shihong Chen*

A novel enhanced electrochemiluminescence (ECL) sensor based on gold nanoflower@g-C₃N₄ nanosheet–polyaniline hybrids was prepared to detect dopamine.

6563

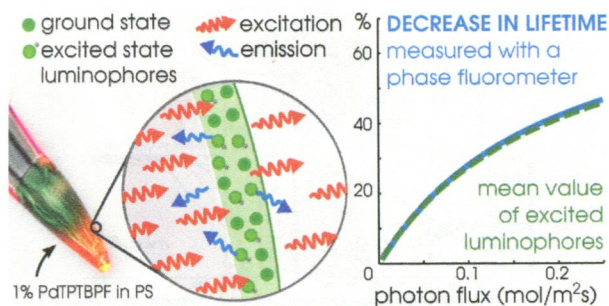


Signal-on electrochemical immunoassay for APE1 using ionic liquid doped Au nanoparticle/graphene as a nanocarrier and alkaline phosphatase as enhancer

Zhaoyang Zhong,* Mengxia Li, Yi Qing, Nan Dai, Wei Guan, Wei Liang and Dong Wang*

In this paper, the Au nanoparticles decorated graphene nanosheets (AuNPs/Gr) were prepared as nanocarriers using ionic liquid (IL) as linker reagent.

6569

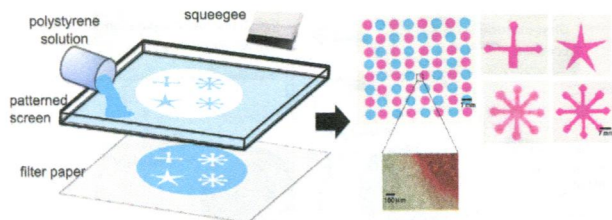


The effect of high light intensities on luminescence lifetime based oxygen sensing

Christoph Larndorfer,* Sergey M. Borisov, Philipp Lehner and Ingo Klimant

This study highlights possible errors in luminescence lifetime measurements when using bright optical oxygen sensors with high excitation light intensities.

6580



One-step polymer screen-printing for microfluidic paper-based analytical device (μPAD) fabrication

Yupaporn Sameenoi,* Piyaporn Na Nongkai, Souksanh Nouanthavong, Charles S. Henry and Duangjai Nacapricha

A new simple, low-cost and one-step method for the fabrication of μPAD using only polystyrene and a patterned screen.

Correction: Ultrasensitive carbohydrate-peptide SPR imaging microarray for diagnosing IgE mediated peanut allergy

Amit A. Joshi, Mark W. Peczuh, Challa V. Kumar and James F. Rusling*

